Materials Letters 228 (2018) 254–257

Contents lists available at ScienceDirect

Materials Letters

journal homepage: www.elsevier.com/locate/mlblue

Microstructure evolution of nonstoichiometric $ZrC_{0.6}$ with ordered carbon vacancies under ion irradiation

Boxin Wei [a,b], Yujin Wang [a,*], Haibin Zhang [b,*], Dong Wang [a], Shuming Peng [b], Yu Zhou [a]

[a] Institute for Advanced Ceramics, School of Materials Science and Engineering, Harbin Institute of Technology, Harbin 150001, China
[b] Innovation Research Team for Advanced Ceramics, Institute of Nuclear Physics and Chemistry, China Academy of Engineering Physics, Mianyang 621900, China

ARTICLE INFO

Article history:
Received 30 March 2018
Received in revised form 29 May 2018
Accepted 6 June 2018
Available online 6 June 2018

Keywords:
Zirconium carbide
Order vacancies
Defects
Radiation damage

ABSTRACT

$ZrC_{0.6}$ with ordered carbon vacancies was irradiated with a 4 MeV Au ion beam at room temperature at fluences of 2×10^{16} ions/cm^2, corresponding to 130 displacements per atom (dpa). Grazing incidence X-ray diffraction and transmission electron microscopy were performed to investigate the microstructure evolution of $ZrC_{0.6}$ under ion irradiation. The lattice parameter did not clearly increase (lattice expansion of 0.013%) for irradiated $ZrC_{0.6}$, which indicated that the inherent carbon vacancies acted as sinks for the interstitial atoms generated by irradiation. The peaks of Zr_2C-ordered phase in GIXRD patterns and reflections of ordered Zr_2C in microdiffraction patterns of the damaged layer disappeared, which indicated that superstructure modulation of the ordered carbon vacancies for Zr_2C was destroyed under Au ion irradiation, and demonstrated that introducing vacancy defects in ZrC enhanced the tolerance of radiation damage.

1. Introduction

In the frame work of Generation-IV nuclear energy systems, zirconium carbide (ZrC) is considered an accident tolerant fuel-particle coating or an inert matrix material because of its high thermal conductivity, low neutron absorption cross-section and excellent resistance to attack by fission products [1,2]. Nonstoichiometric ZrC_x is stable over a wide compositional range and has a high concentration of vacancies according to the Zr-C phase diagram [3]. For nonstoichiometric carbides, disordered carbon vacancies are usually considered to be metastable at room temperature. Long-duration post-annealing or other special sintering techniques are necessary to achieve ordered carbon vacancies [4,5], and it is known that carbon vacancies are a critical factor for investigating the irradiation behavior of ZrC_x [6]. However, the present study focus was limited to the effects of carbon vacancies on ZrC_x evaluation under irradiation [7,8], especially the effects on ordered carbon vacancies.

The purpose of the present work was to investigate the microstructure evolution of nonstoichiometric $ZrC_{0.6}$ with ordered carbon vacancies under ion irradiation. In this study, $ZrC_{0.6}$, with ordered carbon vacancies, was fabricated by a two-step reactive hot pressing process and then irradiated with a 4 MeV Au ion beam at room temperature to fluences of 2×10^{16} ions/cm^2. Grazing incidence X-ray diffraction (GIXRD) and transmission electron microscopy (TEM) were performed to investigate radiation damage and microstructure evolution.

2. Experiment

Nonstoichiometric $ZrC_{0.6}$ with ordered carbon vacancies was successfully fabricated by two-step reactive hot pressing (1500 °C, 30 MPa, and 1 h) as described in our previous studies [9]. The density of the sample was 97.6% and specimens with dimensions of $3 \times 4 \times 5$ mm^3 were cut from hot-pressed samples. Before irradiation, specimen surfaces were polished to a mirror finish. Irradiations were performed on the 5SDH-2 accelerator with 4 MeV gold ions of a fluence of 2×10^{16} ions/cm^2 at room temperature. The number of displacements per atoms (dpa) of target samples after irradiation in the depth was calculated with SRIM 2013 in full cascade mode [10], using Au-ion energy of 4 MeV and displacement energies of 35 and 25 eV for Zr and C, respectively. Damage curves are shown in Fig. 1a. GIXRD (Empyrean, Malvern Panalytical B. V., Almelo, The Netherlands) with CuK_α radiation was used to analyze sample structural modifications from irradiation. TEM (FEI Talos F200x, FEI Co., Hillsboro, OR, USA) was employed for a more detailed microstructure analysis.

* Corresponding authors.
E-mail addresses: wangyuj@hit.edu.cn (Y. Wang), hbzhang@caep.cn (H. Zhang).

https://doi.org/10.1016/j.matlet.2018.06.010
0167-577X/

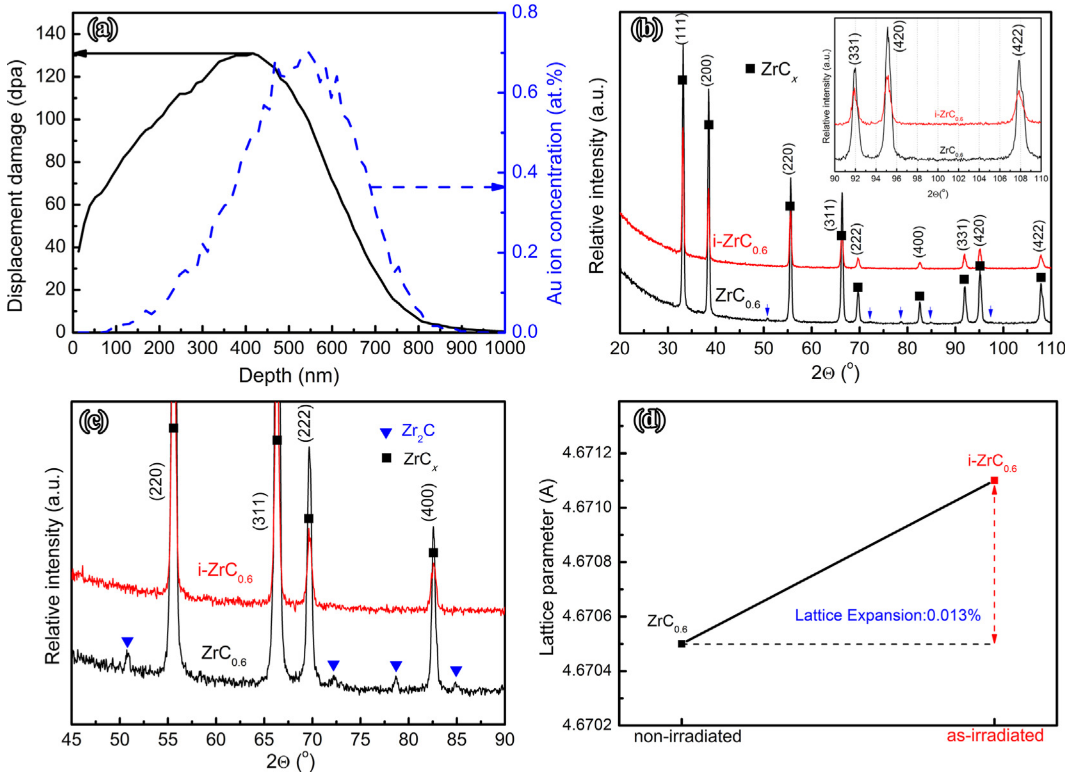

Fig. 1. (a) SRIM estimation of damage for $ZrC_{0.6}$ irradiated with 2×10^{16} ions/cm^2 by a 4 MeV Au ion beam. (b) GIXRD of $ZrC_{0.6}$ before and after irradiation. Inset: patterns at high angle, magnified. (c) Expanded GIXRD of $ZrC_{0.6}$ before and after irradiation. (d) Lattice parameters and lattice expansion of $ZrC_{0.6}$ before and after irradiation.

3. Results and discussion

3.1. Lattice parameter changes

GIXRD patterns of nonirradiated and Au-irradiated surfaces of $ZrC_{0.6}$ samples showed that, before irradiation, the major peaks corresponded to the nonstoichiometric ZrC_x phase with disordered carbon vacancies (Fig. 1b). However, some extra-weak peaks were observed in the enlarged view (Fig. 1c). These extra-weak peaks corresponded to a Zr_2C-type ordered phase that originated from a cubic superstructure of ordered carbon vacancies, as observed in our previous studies [9]. After irradiation, the peaks of Zr_2C-ordered phase disappeared in XRD patterns of i-$ZrC_{0.6}$, demonstrating that ordered carbon vacancies were destroyed under Au ion irradiation. Also, no other miscellaneous peaks were found in the patterns of irradiated $ZrC_{0.6}$, indicating that amorphous transition or decomposition had not occurred in $ZrC_{0.6}$ under irradiation.

Notably, some very small shifts of peaks from high to low angle for $ZrC_{0.6}$ samples before and after irradiation were observed in magnified GIXRD patterns at high angle (Fig. 1b). The decrease in the 2θ angle indicated an increase in the corresponding d-spacing. To acquire a quantitative comparison, the lattice parameters of nonirradiated and irradiated $ZrC_{0.6}$ were calculated from the diffraction data (Fig. 1d). The increment in the lattice parameter of $ZrC_{0.6}$ (lattice expansion of 0.013%) was not significant and far smaller than those of stoichiometric ZrC (lattice expansion 0.128%, under 4 MeV Au irradiation of a fluence of 5×10^{15} ions/cm^2) that has been reported by Gosset et al. [2]. During irradiation, inherent carbon vacancies in $ZrC_{0.6}$ acted as sinks for introduced interstitial atoms generated by irradiation, which restrained lattice expansion.

3.2. Microstructure changes

Within a bright-field (BF) TEM image taken from the nonirradiated $ZrC_{0.6}$ sample (Fig. 2a), a selected area electron diffraction (SAED) pattern obtained from the zone axis of [0 1 1] demonstrated the presence of superstructure modulation and showed the good crystallinity of nonirradiated $ZrC_{0.6}$ (Fig. 2b). Apart from the relatively evident reflections of ZrC_x with NaCl structure, weak superstructural reflections of ordered Zr_2C were observed (Fig. 2b, white arrows). Gusev et al. [11] have constructed a crystal structure model for ordered phase Zr_2C. In the C sublattice, two evident types of $(1\,\bar{1}\,1)_C$ planes were recognized, identified as A and B, respectively. In the $(1\,\bar{1}\,1)_C$ planes of type A, 1/3 of the positions were occupied by C atoms and the rest vacancies, while 2/3 of the positions were occupied by C atoms, with the rest being vacancies in the B-type $(1\,\bar{1}\,1)_C$ planes. The alternate stacking of the A- and B-type $(1\,\bar{1}\,1)_C$ planes generated a Zr_2C-type cubic superstructure along the [1 1 1] direction. According to HRTEM image after Fourier filtering processing and deconvolution (Fig. 2e), the superstructure modulation was clear. The distance of the superstructural ordering planes of $(1\,\bar{1}\,1)$ was detected to be 0.544 nm, which was precisely two times the distance of the face-centered cubic (fcc) $(1\,\bar{1}\,1)$ planes.

The cross-section BF-TEM image of $ZrC_{0.6}$ after irradiation is shown in Fig. 3a, in which a red arrow highlights the implant direction and white lines show the damage surface and depth. The depth of the distinct damage layer was observed to be 900 nm, which matched with SRIM simulations. A BF-TEM image of the damaged area interior in irradiated $ZrC_{0.6}$ showed that the irradiated microstructure was dominated by a large number of small black dots (Fig. 3b). No apparent dislocation loops or radiation-induced